Details of Pulsar Wind Nebula Radiative Modeling

Alina Kochocki (University of California, Los Angeles)

This document outlines the modeling of spectral energy distributions for one-zone, leptonically-driven pulsar wind nebulae (PWNe). A set of relevant equations defining the dynamics of the pulsar are introduced. The production and energy budget of the plerion is discussed, and a process is presented to model the electron/positron source energy spectrum as a function of time. The semi-classical approximation for inverse-Compton scattering is introduced, as a well as a numerical approximation for synchrotron production. The resulting PWN energy spectrum as a product of these two radiative mechanisms is then discussed in view of a number of test cases. This text highlights any uncertain claims or discrepancies from the results of other works.

A. Dynamics of PWN Evolution

A rotating neutron star, or pulsar, is commonly approximated as a rotating magnetic dipole. The energy loss rate, or spin-down power relies on the angular velocity, Ω, as described in [1] (H.E.S.S. PWN Survey):

$$\dot{E} = -k'\Omega^4. \tag{1}$$

Here, k' is some constant of proportionality. The change in angular momentum is:

$$\dot{J} = \frac{\dot{E}}{\Omega} = k'\Omega^3. \tag{2}$$

For I, the moment of inertia of the neutron star, the angular velocity loss rate is:

$$\dot{\Omega} = \frac{\dot{J}}{I} = -k\Omega^3. \tag{3}$$

In the general case where other factors beyond magnetic braking may contribute, the index of 3 is set to the braking index, n. Finally, the differential equation described may be solved for $\Omega(t)$:

$$\Omega(t) = \Omega_0\left(1 + \frac{t}{\tau_0}\right)^{\frac{1}{1-n}}. \tag{4}$$

Here, τ_0 is the initial spin-down timescale. From this expression, the following relationships describing the dynamical evolution of a rotating body undergoing some form of braking can be derived as below:

$$\dot{E}(t) = \dot{E}_0 \left(1 + \frac{t}{\tau_0}\right)^{\frac{n+1}{1-n}}, \tag{5}$$

where $\dot{E}_0$ is the initial spin-down power (at $t = 0$). Relating $\Omega(t)$ to the period of rotation, $P = 2\pi/\Omega$:

$$P(t) = P_0 \left(1 + \frac{t}{\tau_0},\right)^{\frac{1}{n-1}}, \tag{6}$$

then differentiating:

$$\dot{P}(t) = \frac{P_0}{\tau_0(n-1)} \left(1 + \frac{t}{\tau_0}\right)^{\frac{2-n}{n-1}}. \tag{7}$$

Finally, the characteristic lifetime, $\tau_c(t)$, is expressed as below:

$$\tau_c(t) = \frac{P(t)}{2\dot{P}(t)} = \frac{n-1}{2}(t + \tau_0). \tag{8}$$

The magnetic field strength is also described as a function of time:

$$B(t) = \frac{B_0}{1 + \left(\frac{t}{\tau_0}\right)^{\alpha}} + B_{\rm ISM}. \tag{9}$$

Here, $B_{\rm ISM}$ is the constant contribution of the ISM, unassociated with the dynamics of the PWN. Last, drawing on analytical studies of expanding PWNe, the plerion radius has been described as a function of time for two cases. First, when the reverse shock interaction time ($t_{\rm rs}$), is greater than τ_0:

$$R(t) \propto \begin{cases} t^{6/5} & \text{for } t \leq \tau_0 \\ t & \text{for } \tau_0 < t \leq t_{\rm rs} \\ t^{3/10} & t > t_{\rm rs}. \end{cases} \tag{10}$$

$$\dot{R}(t) \propto \begin{cases} \frac{6}{5}t^{1/5} & \text{for } t \leq \tau_0 \\ 1 & \text{for } \tau_0 < t \leq t_{\rm rs} \\ \frac{3}{10}t^{-7/10} & t > t_{\rm rs}. \end{cases} \tag{11}$$

$$\ddot{R}(t) \propto \begin{cases} \frac{6}{25}t^{-4/5} & \text{for } t \leq \tau_0 \\ 0 & \text{for } \tau_0 < t \leq t_{\rm rs} \\ -\frac{21}{100}t^{-17/10} & t > t_{\rm rs}. \end{cases} \tag{12}$$

$$\tau_{\rm ad}(t) = \begin{cases} \frac{15}{4}t & \text{for } t \leq \tau_0 \\ \frac{3}{2}t & \text{for } \tau_0 < t \leq t_{\rm rs} \\ -30t & t > t_{\rm rs}. \end{cases} \tag{13}$$

The radius of the PWN must be specified at some time, then the proportionality constants for each epoch determined to satisfy continuity. In the case the reverse shock interaction time is less than τ_0:

$$R(t) \propto \begin{cases} t^{6/5} & \text{for } t \leq t_{\rm rs} \\ t^{11/15} & \text{for } t_{\rm rs} < t \leq \tau_0 \\ t^{3/10} & t > \tau_0. \end{cases} \tag{14}$$

In the study performed by the H.E.S.S. collaboration in [1], these above relations are used to model the radiative and dynamic evolution of the PWN as a function of time. A set of characteristic parameters presented in this section are defined for a rotating magnetic dipole, the 'baseline model', or archetypal PWN. In addition, a range of parameters typical of observed PWNe are also provided. These are listed in the table below.

Variable Name	Variable Character	Baseline Value	Varied Range
Braking index	n	3.0	2.5..3.5
Initial spin-down power	$\dot{E}_0$ (10^{39}erg s^{-1})	2.0	1.0..4.0
Initial spin-down timescale	τ_0 (kyr)	0.5	0.32..0.77
Initial magn. field strength	B_0 (G)	200	110..270
Reverse shock interaction timescale	$t_{\rm rs}$ (kyr)	4.0	4.0..8.0
PWN radius ($t = 3$ kyr)	R_3 (pc)	6.0	3.0..12.0
ISM magn. field strength	$B_{\rm ISM}$ (G)	3.0	3.0
Index of magn. field evolution	α	0.6	0.6

The dynamical expressions of this section were evaluated for the archetypal PWN as a function of time, and shown to match the results tabulated in [1]. It should be noted, all of these results are independent of P_0, as it cancels in calculation of τ_c, where $P(t)$ and $\dot{P}(t)$ are used in modeling.

B. Modeling of the Leptonic Spectrum

The energy spectrum of leptons is determined from two processes within the PWN nebula, the 'cooling' of particles (energy loss), and the injection of fresh leptons with energy provided by the spin-down of the pulsar. The resulting spectrum is described by the transport equation:

$$\frac{dN}{dE}(E, t + \delta t) = \frac{dN_{\rm cooled}}{dE}(E, t) + \frac{dN_{\rm inj}}{dE}(E, t + \delta t). \tag{15}$$

Here, the term $dN_{\rm inj}/dE$ describes the spectrum of newly injected particles in the time δt. As the pulsar ages and its period increases, the loss in rotational energy described by $\dot{E}$ is converted to a spectrum of high energy electrons and positrons within the pulsar wind nebula. The amount of spin-down energy attributed to these particle fields can be determined in a time δt of the pulsar's lifetime, T:

$$E_p(t) = \eta \int_t^{t+\delta t} \dot{E}(t) dt. \tag{16}$$

Here, η describes the conversion efficiency from rotational to particle energies. To follow the procedure set out in [1], η will be set as unity for all modeling purposes. This E_p sets an energy budget for the integral energy contained in newly injected leptons. Assuming these new particles

follow a power law distribution:

$$\frac{dN_{\rm inj}}{dE}(E,t) = \Phi_0(t)\Big(\frac{E}{1\ \rm TeV}\Big)^{-\beta}. \tag{17}$$

Equating the integral energy held in leptons with that delivered from spin-down:

$$\frac{1}{\Phi_0(t)} = \frac{1}{E_p(t)}\int_{\rm E_{min}}^{\rm E_{max}} E\Big(\frac{E}{1\ \rm TeV}\Big)^{-\beta} dE. \tag{18}$$

$\rm E_{min}$ and $\rm E_{max}$ are chosen as 30 GeV and 300 TeV, respectively. $\rm E_{min}$ and $\rm E_{max}$ also define the limits of the total spectrum, dN/dE. The extra factor of E under the integral should also be noted (present in [2], but not [1]).

The term $dN_{\rm cooled}/dE$ describes the differential cooling of the spectrum:

$$\frac{dN_{\rm cooled}}{dE}(E,t) = \frac{dN}{dE}(E, t-\delta t)\cdot \exp\Big(-\frac{\delta t}{\tau_{\rm eff}(E,t)}\Big). \tag{19}$$

Specifically, since the last time step, the entire spectrum, dN/dE, has decreased in magnitude due to cooling losses. The flux for a given value of energy has decreased exponentially, with a characteristic timescale ($\tau_{\rm eff}$), determined by time and energy. The injection of new particles offsets this process, but is only a viable mechanism while the rate of spin-down is still high (hence the dominance of young pulsars associated with observable GeV-TeV PWN).

The cooling timescale, $\tau_{\rm eff}$ is given by:

$$\tau_{\rm eff}^{-1} = \tau_{\rm syn}^{-1} + \tau_{\rm esc}^{-1} + \tau_{\rm ad}^{-1}. \tag{20}$$

The synchrotron and escape losses are described by:

$$\tau_{\rm syn}(E,t) = 12.5\cdot\Big[\frac{B(t)}{10\ \mu\rm G}\Big]^{-2}\cdot\Big[\frac{E}{10\ \rm TeV}\Big]^{-1}\rm kyr, \tag{21}$$

$$\tau_{\rm esc}(E,t) = 34\cdot\Big[\frac{B(t)}{10\ \mu\rm G}\Big]\cdot\Big[\frac{E}{10\ \rm TeV}\Big]^{-1}\Big[\frac{R(t)}{1\ \rm pc}\Big]^{2}\rm kyr. \tag{22}$$

These values are straightforward to evaluate, with $R(t)$ and $B(t)$ as defined in the previous section. Beyond these two timescales, which are included in the following work, [1] claims to incorporate both an adiabatic cooling timescale, and an additional timescale due to losses associated with

inverse-Compton (IC) processes. These two processes are not yet implemented. [1] suggests subtracting the IC emissivity as a function of energy for each δt considered. The adiabatic loss timescale is described as:

$$\tau_{\rm ad}(E,t) = -\frac{E}{\dot{E}_p} = \frac{3}{\nabla \mathbf{v}_\perp(R)}, \tag{23}$$

$$\nabla \mathbf{v}_\perp(R) = \frac{1}{R(t)^2} \cdot \frac{\partial (R(t)^2 \mathbf{v}_\perp(t))}{\partial t} \cdot \frac{\partial t}{\partial R}, \tag{24}$$

$$\nabla \mathbf{v}_\perp(R) = \frac{1}{\dot{R(t)} R(t)^2} \cdot \frac{\partial (R(t)^2 \dot{R(t)})}{\partial t}, \tag{25}$$

$$\nabla \mathbf{v}_\perp(R) = \frac{1}{\dot{R(t)} R(t)^2} \cdot \left(2R(t)\dot{R(t)}^2 + \ddot{R(t)} R(t)^2 \right). \tag{26}$$

This likely suggests there is some canonical expression for a particle's velocity within the PWN, making the radial component, $\mathbf{v}_\perp$, well defined. This is not investigated further in this work.

To determine $dN(E)/dE$ for a pulsar of age T, this age is divided into a number of equally spaced time-steps, each of duration δt. In the first time-step, the first population of injected leptons is determined, and set equal to dN/dE. In the second step, an additional population is added, while the existing has experienced cooling losses. This process continues until a time T is reached.

[1] again provides nominal and varied values for the variables used in this modeling:

Variable Name	Variable Character	Baseline Value	Varied Range
Lepton conversion efficiency	η	1.0	1.0
Index of lepton injection spectrum	β	2.0	1.75..2.25
Minimum Energy of Lepton Distribution	$\mathrm{E_{min}}$ (TeV)	0.03	0.03
Maximum Energy of Lepton Distribution	$\mathrm{E_{max}}$ (TeV)	300	300

In [1], the set of baseline parameters described in the two tables of this work are used to model a PWN leptonic spectrum, and then to find total radiative output due to synchrotron and inverse-Compton processes. Following the procedure and parameters outlined above, the resulting leptonic spectrum with varying age is shown below.

The results of this modeling appear physical, but have not yet been validated to be the exact input leptonic spectrum used in [1].

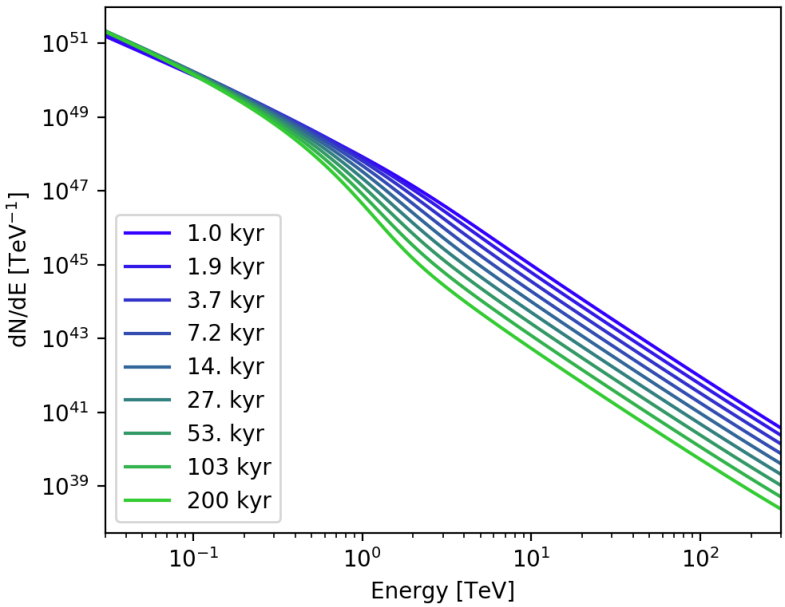

FIG. 1: "Baseline PWN Leptonic Energy Spectrum": Shown above is the leptonic energy spectrum for a PWN modeled with 'baseline' model parameters. The spectrum is plotted as a function of pulsar age. The magnitude and evolution of the spectrum appears compatible with similar modeling performed in other works [2].

C. Modeling of Radiative Mechanisms/Production

In this section, two models for inverse-Compton scattering and synchrotron radiation are presented. Any necessary details about their implementation or evaluation are described. Some background is provided, but the forms are not derived in this text.

Both mechanisms presented here are functions of the leptonic spectrum derived in the previous section (this is a PWN-specific model). Lower energy photons produced in PWNe are associated with the process of synchrotron. The emissivity for synchrotron is modeled in [3] and expressed as:

$$\frac{dN}{dE_\gamma dt} = \frac{\sqrt{3}}{2\pi} \frac{e^3 B}{m_e c^2 \hbar E_\gamma} F\left(\frac{E_\gamma}{E_c}\right), \tag{27}$$

where,

$$F(x) = x \int_x^\infty K_{5/3}(\tau) d\tau, \tag{28}$$

$$E_c = \frac{3e\hbar B\gamma^2}{2m_e c}. \tag{29}$$

Here, e, m_e and c refer to electron charge, mass and the speed of light. $B(t)$ is the magnetic field strength as described in the first section. E_γ is the value of photon energy corresponding to $dN/dE_\gamma dt$. γ describes the Lorentz factor of an electron. To account for the physical nature of the PWN, it is assumed that magnetic fields are oriented randomly, and a second integral over the angle between $\mathbf{B}$ and particle velocity, $\mathbf{v}$, may be performed. This results is a function of Bessel functions, but can be approximated [3], below as:

$$\frac{dN}{dE_\gamma dt} = \frac{\sqrt{3}}{2\pi}\frac{e^3 B}{m_e c^2 \hbar E_\gamma}\frac{1.808x^{1/3}}{\sqrt{1+3.4x^{2/3}}}\frac{1+2.21x^{2/3}+0.347x^{4/3}}{1+1.353x^{2/3}+0.217x^{4/3}}e^{-x} \tag{30}$$

This approximation has been shown to agree with the nominal function for emissivity to within 0.2% over all x. To account for a distribution of electrons, the final radiative spectrum is determined from:

$$\left(\frac{dN_{\rm tot}}{dE_\gamma dt}\right)_{\rm syn} = \int_{\gamma_{\rm min}}^{\gamma_{\rm max}} N_{\rm e}(\gamma)\frac{dN}{dE_\gamma dt}(\gamma)d\gamma \tag{31}$$

Here, $\gamma_{\rm min}$ and $\gamma_{\rm max}$ correspond to $\rm E_{min}$ and $\rm E_{max}$ presented in the last section, ($\gamma_{\rm min} = \rm E_{min}/m_e c^2$). $N_{\rm e}$ is such that $N_{\rm e}(\gamma)d\gamma = dN_e$, placing the leptonic energy spectrum of the previous section (dN/dE), in units of electron rest energy. The resulting synchrotron distribution has been shown to agree with Naima for a test leptonic distribution.

Inverse-Compton processes are modeled following the semi-classical approximation for emissivity. The specific form has been referenced from [4,2], which is also cited by [1]. A target photon field with differential density described by:

$$n(\varepsilon) = \frac{dn}{d\varepsilon dV}, \tag{32}$$

is considered. ε is the energy of target photons. It can be shown,

$$\left(\frac{dN_\varepsilon}{dE_\gamma dt}\right)_{\rm IC} = \frac{2\pi r_e^2 m_e c^3}{\gamma}\frac{n(\varepsilon)d\varepsilon}{\varepsilon}\left[2q{\rm ln}q + (1+2q)(1-q) + \frac{1}{2}\frac{(\Gamma_e q)^2}{1+\Gamma_e q}(1-q)\right], \tag{33}$$

where, $\Gamma_e = 4\varepsilon\gamma/m_e c^2$, $q = E_1/\Gamma_e(1-E_1)$, and the energy of the up-scattered photon, E_γ, is such that $E_\gamma = E_1\gamma m_e c^2$. Certain physical bounds are placed on these parameters, described in [4]. Again, this equation is evaluated at only one electron energy ($\gamma m_e c^2$), and a single target photon

energy, ε. The subscript, ε, has been used to denote this, while γ has been dropped to discourage confusion between the Lorentz factor and up-scattered photon subscript. The total spectrum from IC processes is found by integrating over the entire leptonic spectrum and target photon field distributions:

$$\left(\frac{dN_{\rm tot}}{dE_\gamma dt}\right)_{\rm IC} = \int_{\varepsilon_{\rm min}}^{\varepsilon_{\rm max}} \int_{\gamma_{\rm min}}^{\gamma_{\rm max}} N_{\rm e}(\gamma) \frac{dN_\varepsilon}{dE_\gamma dt}(\gamma, \varepsilon) d\gamma d\varepsilon \tag{34}$$

Finally, the total spectral energy distribution for a leptonically driven PWN is:

$$\left(\frac{dN_{\rm tot}}{dE_\gamma dt}\right) = \left(\frac{dN_{\rm tot}}{dE_\gamma dt}\right)_{\rm IC} + \left(\frac{dN_{\rm tot}}{dE_\gamma dt}\right)_{\rm syn}. \tag{35}$$

Currently, for a test leptonic distribution and CMB photon field, Naima results, and the implementation of the above expression for inverse-Compton do not agree. The shape is somewhat similar over the same relevant decades in energy, but the normalization is clearly off by several orders of magnitude. Naima uses a different approximation for IC, which may partially contribute, however a test case presented in [2] also disagrees.

As the integration over the leptonic energy spectrum is performed the same as in the case of synchrotron, there is likely some error with the target CMB photon field input, or its integration.

Beyond these test cases, radiative production (synchrotron only), for the case of the leptonic distribution derived in the previous section was also attempted. Results presented in [1] for both synchrotron and IC are compared to these results below (FIG. 2 FIG. 3).

There is clearly some additional discrepancy between the modeled leptonic spectrum, and that used in [1].

Finally, some preliminary results for modeling of inverse-Compton are included. Again, the leptonic distribution modeled in this work is used as input. The target photon field is defined by the number density of a black body emitter at $T = 2.725$ K:

$$n_\nu d\nu = \frac{8\pi\nu^2}{c^3} \frac{1}{\exp(h\nu/kT) - 1} d\nu \tag{36}$$

In this case, the range of frequencies bounding the relevant portion of this distribution are integrated over in place of energy.

The the resulting radiative distribution (FIG. 4) is relatively high in magnitude compared to the synchrotron component. This feature was identified in other test cases independent of the leptonic distribution discussed here. Similar behavior with age is observed when compared to the

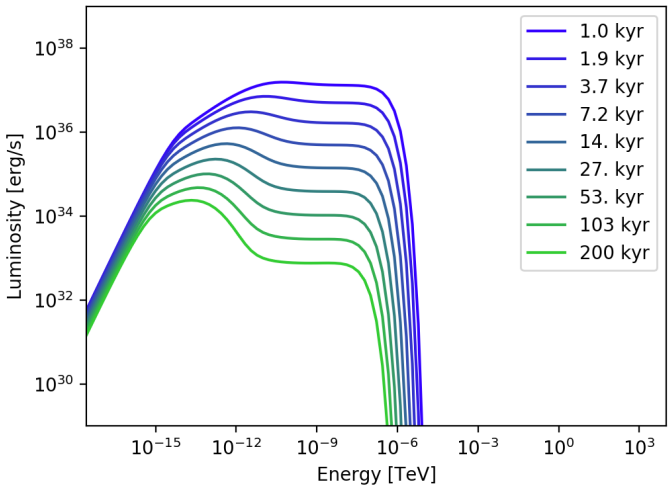

FIG. 2: "Baseline PWN Synchrotron Spectral Energy Distribution": Pictured above is the radiative spectrum produced by synchrotron as determined in this work. Inverse-Compton contributions are not shown.

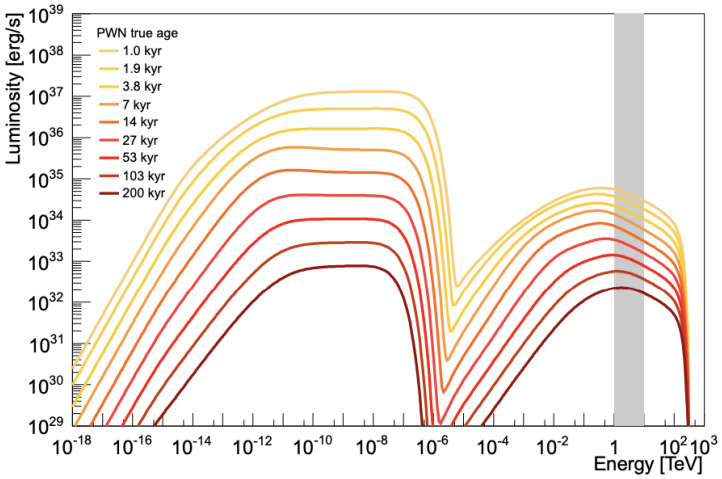

FIG. 3: "Baseline PWN Spectral Energy Distribution (H.E.S.S)": Shown above is the total spectral energy distribution as determined by H.E.S.S in [1]. The results of synchrotron radiative production clearly differ from those in FIG. 2.

synchrotron spectrum modeled in this work. It is likely that in both cases, there is some problem in modeling the lower-energy end of the leptonic spectrum.

D. Future Work

There are a number of items left to consider in recreating the modeling of [1]. First, the cooling timescale due to adiabatic losses, and the energy loss or impact of inverse-Compton processes should

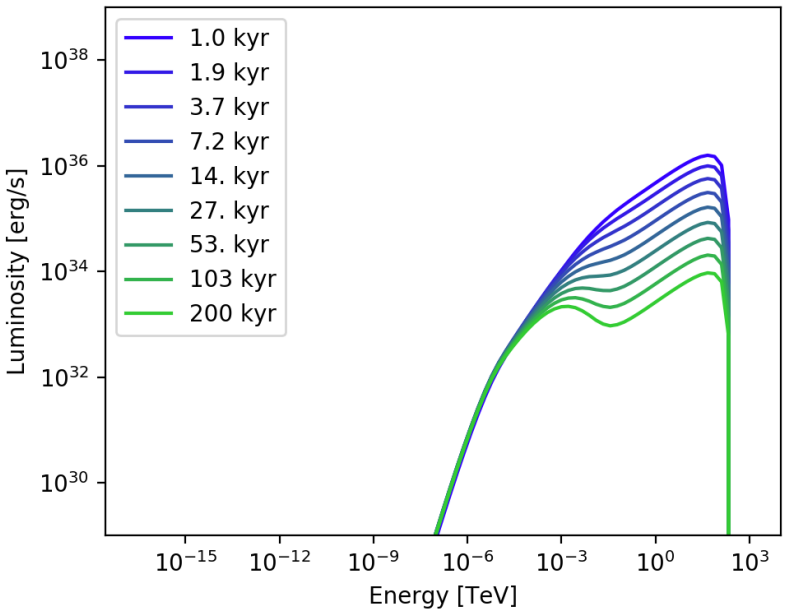

FIG. 4: "Baseline PWN Inverse-Compton Spectral Energy Distribution": Pictured is the inverse-Compton radiative spectrum for a PWN with 'baseline' model parameters. The spectrum is again plotted as a function of pulsar age.

be investigated and factored in to the term dN_{cooled}/dE. Second, the modeling of inverse-Compton radiative production needs to be validated in some test case. It is most likely that there is some problem with the input photon field, and the differential density of the CMB should be confirmed. Eventually, GALPROP values for a source's galactic location will need to be referenced, as in [1]. Finally, the modeled leptonic spectrum must be shown to be accurate to the description in this text. This would either be performed after making the above adjustments and successfully recreating the results of [1], or possibly diagnosing some alternate error in its scripted implementation.

---

[1] H. Abdalla, A. Abramowski, F. Aharonian, F. Ait Benkhali, A. G. Akhperjanian, T. Andersson, E. O. Angüner, M. Arrieta, P. Aubert, and et al. The population of tev pulsar wind nebulae in the h.e.s.s. galactic plane survey. Astronomy Astrophysics, 612:A2, Apr 2018.

[2] M. Mayer. Phd thesis, u. erlangen-nuremberg (main). 2010.

[3] F. A. Aharonian, S. R. Kelner, and A. Yu. Prosekin. Angular, spectral, and time distributions of highest energy protons and associated secondary gamma rays and neutrinos propagating through extragalactic magnetic and radiation fields. Physical Review D, 82(4), Aug 2010.

[4] GEORGE R. BLUMENTHAL and ROBERT J. GOULD. Bremsstrahlung, synchrotron radiation, and compton scattering of high-energy electrons traversing dilute gases. Rev. Mod. Phys., 42:237–270, Apr 1970.